

Spins, shapes, and orbits for near-Earth objects by Nordic NEON

Karri Muinonen¹†, Johanna Torppa¹, Jenni Virtanen¹, Jyri Näränen¹,
Jarkko Niemelä¹, Mikael Granvik¹, Teemu Laakso¹,
Hannu Parviainen¹, Kaare Aksnes², Zhang Dai²,
Claes-Ingvar Lagerkvist³, Hans Rickman³, Ola Karlsson³,
Gerhard Hahn⁴, René Michelsen⁵, Tommy Grav⁶, Petr Pravec⁷,
and Uffe Gråe Jørgensen⁸

¹Observatory, Kopernikuksentie 1, P.O. Box 14, FI-00014 University of Helsinki, Finland
email: Karri.Muinonen@helsinki.fi

²University of Oslo, Institute of Theoretical Astrophysics, PB 1029 Blindern, 0315 Oslo, Norway

³Uppsala Astronomical Observatory, Box 515, S-75120 Uppsala, Sweden

⁴German Aerospace Center (DLR), Institute of Planetary Research, Rutherfordstrasse 2, D-12489 Berlin, Germany

⁵Ørsted DTU, Technical University of Denmark, Elektrovej, bldg. 327, DK-2800 Kgs. Lyngby, Denmark

⁶University of Hawaii, Institute for Astronomy, 2680 Woodlawn Drive, Honolulu, Hawaii 96822-1897, USA

⁷Astronomical Institute AV CR, Fricova 298, 25165 Ondrejov, Czech Republic

⁸Astronomical Observatory, Niels Bohr Institute, Juliane Maries Vej 30, DK-2100 Copenhagen, Denmark

Abstract. The observing program of the Nordic Near-Earth-Object Network (NEON) accrues knowledge about the physical and dynamical properties of near-Earth objects (NEOs) using state-of-the-art inverse methods. Photometric and astrometric observations are being carried out at the Nordic Optical Telescope. Here, the NEON observations from June 2004–September 2006 are reviewed. Statistical orbital inversion is illustrated by the so-called Volume-of-Variation method. Statistical inversion for spins and shapes is carried using a simple triaxial shape model yielding analytical disk-integrated brightnesses for both Lommel-Seeliger and Lambert scattering laws. The novel approach allows spin-shape error analyses with the help of large numbers of sample solutions. Currently, such spin-shape solutions have been derived for 2002 FF₁₂, 2003 MS₂, 2003 RX₇, and 2004 HW. For (1862) Apollo, an unambiguous spin-shape solution has been obtained using the conventional, convex inversion method and, for (1685) Toro and (1981) Midas, the conventional method has been applied repeatedly to map the regime of possible solutions.

Keywords. Identification; statistical methods; data analysis; astrometry; photometry; asteroid, rotation; asteroid, lightcurves

1. Introduction

The Near-Earth-Object Network (NEON) carries out coordinated observations of NEOs in order to contribute to the study of their physical and dynamical properties;

† Present address: Observatory, Kopernikuksentie 1, P.O. Box 14, FI-00014 University of Helsinki, Finland.

at the moment we concentrate on photometric and astrometric observations, yielding spin states, shapes, and orbits for NEOs. NEON was initiated by the Nordic Group for Small Planetary Bodies (NGSPB) which represents collaboration between asteroid and comet researchers from mainly Nordic countries. The vast majority of NEON observations have been carried out at the Nordic Optical Telescope (NOT) which is a 2.56-m telescope located at Roque de los Muchachos on La Palma (Canary Islands, Spain).

In the photometric part of the NEON program, the first and second priorities are given to potentially hazardous NEOs with and without earlier photometric data, respectively, whereas the third priority is given to NEOs with earlier photometric data. Note that NOT allows photometric observations and spin-shape analyses of faint fast-moving objects, thus extending the NEO physical studies towards smaller objects.

The primary objective of the astrometric part of the NEON program is the recovery and follow-up of faint potentially hazardous NEOs, that is, securing orbits for critical objects with short observational arcs. Astrometric observations are carried out both for potentially hazardous NEOs not observed lately, which are thus difficult to recover, and for newly discovered objects at risk of becoming lost. Accurate orbit computation is needed both for evaluating the potential collision risk as well as for planning the photometric observations.

During April 2004–September 2006, the total amount of visitor-mode observing time has consisted of 37 nights, of which 27 have been photometric. The visitor-mode time has been mainly used for photometric lightcurve observations. In addition, roughly once a month, two-hour-long service mode/target-of-opportunity observation time slots have been used for astrometric observations of faint NEOs. The service-mode time of $31 \times 2 = 62$ hours has yielded over 40 useful hours for astrometry. For more information about the NEON observing program, we refer the reader to Torppa, Virtanen & Muinonen *et al.* (2006).

The statistical inversion of asteroid astrometric observations for orbits has been reviewed by Howell, Virtanen, Muinonen, *et al.* (2002) and Virtanen, Tancredi, Bernstein *et al.* (2006). They provide methods for objects observed over short, moderate as well as long time intervals. In particular, for moderate time intervals, Muinonen, Virtanen, Granvik *et al.* (2006) have recently offered a solution using what they called volumes of variation in the six-dimensional orbital-element phase space.

The inversion of asteroid photometric observations for spins, shapes, and overall scattering properties of the surfaces have been reviewed by Kaasalainen, Mottola & Fulchignoni (2002). Whereas the convex inversion method – hereafter referred to as the conventional method – is currently well matured and shown to yield realistic spin and shape solutions, the error analysis of the spin-shape solutions, in particular, is still in its infancy: steps towards a statistical treatment of the inverse problem are taken in the present article.

In Sect. 2, we present the NEON observing program with a summary of the photometric and astrometric observations made so far. Section 3 includes the orbital inverse methods and highlights of their application to NEON astrometry, in particular, in connection to NEON recoveries. Section 4 presents the inverse methods for spins and shapes, culminating, on one hand, in the statistical inversion of single-lightcurve data and, on the other hand, on the conventional inversion of the spin and shape for (1862) Apollo. We close the article by conclusions and future prospects in Sect. 5.

2. Nordic-Optical-Telescope Observations

2.1. Photometry

We have carried out the observations using the Andalucia Faint Object Spectrograph and Camera (ALFOSC), which is a 2048×2048 CCD camera with an effective field-of-view of $\sim 6' \times 6'$. We have used the Bessell R-filter for the observations. It provides the best signal since asteroids are mainly at their brightest in the R-band. In addition, we have used 2×2 binning of the pixels to increase the signal-to-noise ratio (S/N) and to decrease the readout times. Care has been taken that no photometric pixel undersampling occurs even with extraordinary seeing conditions.

In the present paper, we include those photometric lightcurve observations in June 2004–September 2006 that have provided more accurate or new results for the spin states of NEOs. Three of our objects – (1685) Toro, (1862) Apollo, and (1981) Midas – have observations published by Lagerkvist, Piironen & Erikson (2001) and by Torppa & Muinonen (2005), and four – 2002 FF₁₂, 2003 MS₂, 2003 RX₇, and 2004 HW – have no earlier lightcurve observations. For example, Figure 4 depicts the lightcurve observed for 2003 MS₂.

When selecting objects for each observing run, there are three particular issues to be considered: (1) A lightcurve provides new information about the object if it significantly increases the total time range of observations, since the longer the total time range is, the more accurate period determination we get; (2) in addition, for shape and spin axes determination we need observations carried out at different observing geometries, i.e., we need to observe the asteroid from both its northern and southern hemispheres – this is ensured by observing the object at different Earth-centered ecliptic longitude and latitude; (3) shape information is also increased when we have observations from a wide range of phase angles, since shadowing effects become more dominant at large phase angles.

The observations included here are tabulated in Table I. We have mainly used relative photometry (i.e., used field stars as a reference for brightness change in the object) due to its simplicity and the weather conditions not being acceptable for absolute photometry throughout the night. However, we have also observed appropriate Landolt photometric standard stars whenever reasonable.

For spin state and shape determination, relative photometry is sufficient, provided that the weather conditions remain stable for at least half the rotation of the object and that the object remains visible. In the case where the period of the object is long, and half the period cannot be covered during one night, absolute photometry is required to be able to obtain a full lightcurve.

2.2. Astrometry

For the follow-up and recovery observations of NEOs, we have been running a monitoring program (corresponding to observatory code J50) that has mostly been operated in service mode but including also observations carried out during the visitor runs. The service mode observations have been obtained in two-hour slots on a monthly basis. Using ALFOSC with 2×2 binning has allowed efficient use of the two-hour runs by providing fast pointing and read-out times combined with acceptable astrometric accuracies (on the 0.1-arcsec level).

Our observing strategy has been to concentrate on the faint end of objects that are not likely to be observed by most amateur telescopes or automated surveys with relatively bright limiting magnitude (around $V = 20$ mag), but which provide the bulk of NEO observations. Highest priority has been given to potentially hazardous objects. Thus,

Table 1. Lightcurves included in the present study (Torppa, Virtanen & Muinonen *et al.* (2006)). All but three curves have been observed at the NOT, one at Dk1.54 and two at Ondrejov. The columns contain the name of the object, date of observation, observing site, phase angle, the filters used and the duration of observations during each night.

Asteroid	Date	Obs site	phase angle	Filters	Duration (h)
(1685) Toro	Jun 18 2004	La Palma, NOT	45	R(rel)	2.9
	Jun 19	La Palma, NOT	45	R(rel)	3.4
	Jun 27	La Silla, Dk1.54	47	R(rel)	3.4
(1862) Apollo	Mar 20 2005	La Palma, NOT	9	R(rel)	3.5
	Mar 31 1998	Ondrejov	5	R	3.5
	Apr 20 1998	Ondrejov	22	R(rel)	3.9
(1981) Midas	Sep 14 2004	La Palma, NOT	26	R(rel)	2.6
	Sep 15	La Palma, NOT	26	R(rel)	4.0
2002 FF12	Sep 16 2004	La Palma, NOT	6	R(rel)	5.8
2003 MS2	Jan 14 2005	La Palma, NOT	17	R(rel)	5.9
2003 RX7	Jun 19 2004	La Palma, NOT	19	R(rel)	6.0
2004 HW	Aug 15 2004	La Palma, NOT	44	R(rel)	3.5
	Aug 17	La Palma, NOT	43	R(rel)	2.3
	Sep 14	La Palma, NOT	22	R(rel)	4.7
	Sep 15	La Palma, NOT	23	R(rel)	4.2
	Sep 16	La Palma, NOT	23	R(rel)	2.7

reasonable object selection is a key part of the observation planning process. To create priority lists of observable NEOs, we have been making use of the orbit computation tools presented below, as well as several web-based asteroid observing services, such as the Lowell Observatory Asteroid Data Services, Minor Planet Center ephemerides, and the ESA Spaceguard Central Node.

For short-arc objects with large sky-plane uncertainties, the above on-line services currently do not give reliable error estimates for the position. Thus, for objects whose positional uncertainties are on the order of, or larger than, the instrument field of view, we rely on our nonlinear methods for uncertainty propagation.

In connection to the astrometric observations, we have obtained altogether 313 Bessell R-filter magnitudes of total 75 objects (data stored in Standard Asteroid Photometric Catalog SAPC <http://www.astro.helsinki.fi/SAPC/>). The magnitudes are instrumental magnitudes that have been corrected for the photometric zero point according to the NOT zero-point monitoring program, but they have not been corrected for extinction, since we do not have standard star observations from the service-mode observations. Also, S/N required for astrometry is not necessarily good enough for reliable photometry. This gives 1- σ error estimates of ± 0.5 mag for the majority of the objects and ± 1.0 mag for the faintest objects ($R > 22$ mag).

2.3. Reductions

The data reductions have been accomplished using IRAF (APPHOT/PHOT and custom-made astrometric routines) and Astrometrica (Raab (2004)). Bias and flat-field corrections were always carried out by using calibration images taken on the same night. For photometry, six to ten reference stars in the field were used to derive the relative magnitudes of the objects. The reference stars were monitored for variability. In the cases

of faint astrometric objects, we utilized the stacking technique, where several images are added to obtain one, more accurate position (higher S/N).

3. Orbits

3.1. Inverse methods

The statistical orbital inversion methods consist of the nonlinear least-squares method with linearized covariances (LSL; *Bowell, Virtanen, Muinonen, et al. (2002), Muinonen & Bowell (1993)*), the Volume-of-Variation method (VoV; *Muinonen, Virtanen, Granvik et al. (2006)*), and orbital ranging (Ranging; *Virtanen, Muinonen & Bowell (2001)* and *Muinonen, Virtanen & Bowell (2001)*). They have been developed in the framework of statistical inversion theory which aims at characterizing the full probability-density functions for the parameters of the inverse problem.

Typically, LSL is applicable to objects with long observational time intervals and large numbers of observations. The solution of the statistical inverse problem is specified by the least-squares orbital elements and their covariance matrix computed at the least-squares point in the orbital-element phase space. It is partly the point-estimate characteristics of LSL that limit its applicability.

VoV offers a cure to the limitations of LSL by mapping the local least-squares solutions in the phase space as a function of one or more of the parameters. The local least-squares solutions of lesser dimensions than the original one allow local sampling of orbital elements. Trial orbital elements qualify for sample elements if they produce statistically acceptable fits to the observational data. VoV is limited by the requirement that partial derivatives need to be computed at the observation dates with subsequent matrix inversion for local covariance matrices. Should the inverse problem be poorly enough defined, VoV runs into difficulties with the matrix inversion.

Ranging offers a rigorous solution to the statistical inverse problem by exploring the full plausible orbital-element phase space for sample orbital elements. By exploring the topocentric ranges and angular elements (Right Ascension and Declination) at two observation dates, Ranging manages to map the full permissible region of the orbital elements without relying on partial derivatives, thus without facing numerical instabilities. Again, trial orbital elements qualify for sample elements if they produce acceptable fits to the data.

3.2. Results

During the course of the program (as of November 2006), four NEOs have been recovered, while improved orbits have been obtained for more than 76 objects. One of the follow-up objects was the PHO 2004 AS₁ whose drastic discovery-night prediction implied a possibility for a short-term (within 48 hours) Earth impact (*Virtanen, Muinonen, Granvik et al. (2005), Virtanen & Muinonen (2006)*) but which was quickly ruled out with new observations. The newly developed VoV technique was tested and proved useful in the follow-up work.

The MBO 2004 QR constitutes a serendipitous discovery by the NEON program. It was discovered on Aug. 15, 2004, and thereafter followed up on Aug. 17 (observational interval of 2 days; 4 observations), Aug. 22 (7 days; 10 observations), and Sept. 16 (31 days; 13 observations). The full observational interval comprises 19 observations over 39 days. Follow-up observations were carried out by making ephemeris predictions from the discovery night onwards using the statistical techniques: Ranging for the first three data sets and VoV for the last.

Figure 1 shows the time evolution of ephemeris predictions with increasing numbers of observations for the MBA 2004 QR discovered and followed up during the NEON

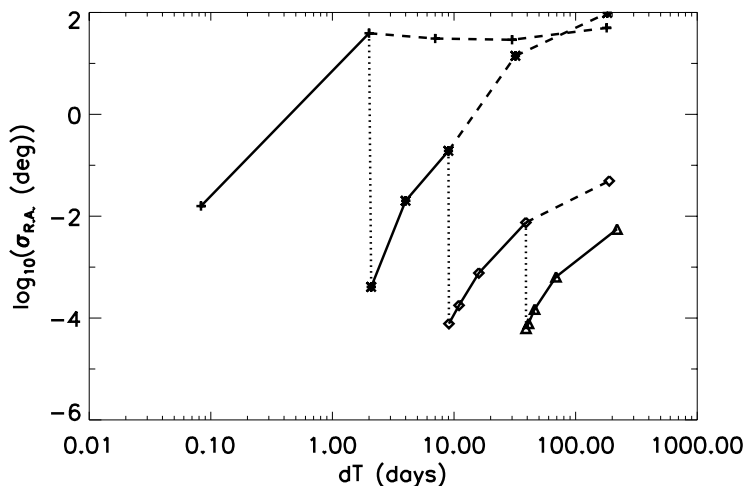


Figure 1. Time evolution of ephemeris uncertainty for 2004 QR. Standard deviation of the R.A. p.d.f.'s as a function of time elapsed from discovery for different lengths of the observational time interval, top to bottom: < 1 day (crosses), 2.0 (stars), 7.2 (diamonds), and 31 days (triangles). Solid-dashed curves show the evolution of ephemeris prediction, dashed part corresponds to the hypothetical evolution without the new observations (timing of which indicated with vertical dotted lines).

program. The collapses (dotted lines) mark the times of the new observations added to the data set. The uncertainty region becomes well-constrained after a week of observations, enabling follow-up observations to be planned for several months ahead. Note the decreasing slope in the increasing ephemeris uncertainty after each time new observations are added.

4. Spins and shapes

4.1. Inverse methods

A simple convex shape model is here constructed from the four quadrants of a sphere, the four halves of two cylinders, and two plane elements (SCyPe; Fig. 2). In the principal-axes reference frame of the shape model, the two plane elements are located on the southern and northern polar regions, being parallel to the equatorial plane defined by the two longest principal axes. The cylinder halves are located on four sides so that their axes are aligned with either one of the two longest axes of the shape. Finally, the four quadrants of the sphere join together the four cylinder halves. There are two parameters in the resulting shape model: the two aspect ratios b/a and c/a among the three principal axes $a \geq b \geq c$. Due to the convexity of the resulting shape, the disk-integrated brightness is simply the sum of the brightnesses from the components, that is, it is an analytical formula consisting of the disk-integrated brightness of the single sphere, the two cylinders, and the two plane elements.

For a semi-infinite plane-parallel medium of scatterers, the reflection coefficient R relates the incident flux density πF_0 and the emergent intensity I as

$$I(\mu, \mu_0, \phi) = \mu_0 R(\mu, \mu_0, \phi) F_0, \quad (4.1)$$

where $\mu_0 = \cos \iota$ and $\mu = \cos \epsilon$, ι and ϵ being the angles of incidence and emergence as measured from the outward normal vector of the surface element, and where ϕ is the

azimuthal angle of emergence (the azimuthal angle of incidence $\phi_0 = \pi$). The Lambert (subscript “L”) and Lommel-Seeliger (“LS”) reflection coefficients are

$$\begin{aligned} R_L(\mu, \mu_0, \phi) &= 1, \\ R_{LS}(\mu, \mu_0, \phi) &= \frac{1}{4} \tilde{\omega} P_{11}(\alpha) \frac{1}{\mu + \mu_0}, \end{aligned} \quad (4.2)$$

where $\tilde{\omega}$ is the single-scattering albedo, P_{11} is the scattering phase function, and α is the phase angle. The Lambert reflection coefficient is applicable to bright scattering media, even though it cannot be derived mathematically from, e.g., the radiative transfer theory. The Lommel-Seeliger reflection coefficient – as the first-order multiple-scattering approximation from the radiative transfer theory – is applicable to dark scattering media: the intensity terms $[\tilde{\omega}^k]$, $k \geq 2$ are assumed negligible. Note that a user-friendly realistic rough-surface scattering model is offered for future work by Parviainen & Muinonen (2006).

The disk-integrated brightness L of an asteroid equals the surface integral (e.g., Muinonen (1998))

$$\begin{aligned} L(\alpha) &= \int_{\iota, \epsilon > 0} dA \mu I(\mu, \mu_0, \alpha) \\ &= \int_{\iota, \epsilon > 0} dA \mu \mu_0 R(\mu, \mu_0, \alpha) F_0. \end{aligned} \quad (4.3)$$

For an irregularly shaped asteroid, L depends on the orientation of the asteroid with respect to the scattering plane, where L is measured.

The plane-element disk-integrated brightnesses for the Lambert and Lommel-Seeliger scattering laws follow, in a straightforward way, from Eqs. 4.2 and 4.3. For a spherical object (diameter D) with Lambert and Lommel-Seeliger reflection coefficients, the disk-integrated brightnesses are

$$\begin{aligned} L_{Ls}(\alpha) &= \frac{1}{6\pi} \pi F_0 D^2 [\sin \alpha + (\pi - \alpha) \cos \alpha], \\ L_{LSs}(\alpha) &= \frac{1}{32} \pi F_0 D^2 \tilde{\omega} P_{11}(\alpha) \left[1 - \sin \frac{1}{2} \alpha \tan \frac{1}{2} \alpha \ln \left(\cot \frac{1}{4} \alpha \right) \right]. \end{aligned} \quad (4.4)$$

For a cylindrical envelope (diameter D and length h , cylinder ends excluded) in its own natural reference frame ($x'y'z'$; with its axis along the z' -axis) and with Lambert and Lommel-Seeliger reflection coefficients, we obtain the disk-integrated brightnesses

$$\begin{aligned} L_{Lc}(\alpha) &= F_0 \frac{1}{2} Dh \left[(\epsilon'_x \iota'_x + \epsilon'_y \iota'_y) \frac{1}{2} (\phi_2 - \phi_1) + (\epsilon'_x \iota'_x - \epsilon'_y \iota'_y) \frac{1}{4} (\sin 2\phi_2 - \sin 2\phi_1) \right. \\ &\quad \left. - (\epsilon'_x \iota'_y + \epsilon'_y \iota'_x) \frac{1}{4} (\cos 2\phi_2 - \cos 2\phi_1) \right], \\ L_{LSc}(\alpha) &= \frac{1}{4} \tilde{\omega} P_{11}(\alpha) F_0 \frac{Dh}{2A} \\ &\quad \cdot \left[C_1 (\sin \lambda_2 - \sin \lambda_1) - C_2 (\cos \lambda_2 - \cos \lambda_1) + C_3 \ln \frac{\cot(\frac{\pi}{4} - \frac{1}{2} \lambda_2)}{\cot(\frac{\pi}{4} - \frac{1}{2} \lambda_1)} \right], \\ A &= \sqrt{(\epsilon'_x + \iota'_x)^2 + (\epsilon'_y + \iota'_y)^2}, \quad \cos \tilde{\phi} = \frac{\epsilon'_x + \iota'_x}{A}, \quad \sin \tilde{\phi} = \frac{\epsilon'_y + \iota'_y}{A}, \\ \lambda_{1,2} &= \phi_{1,2} - \tilde{\phi}, \end{aligned} \quad (4.5)$$

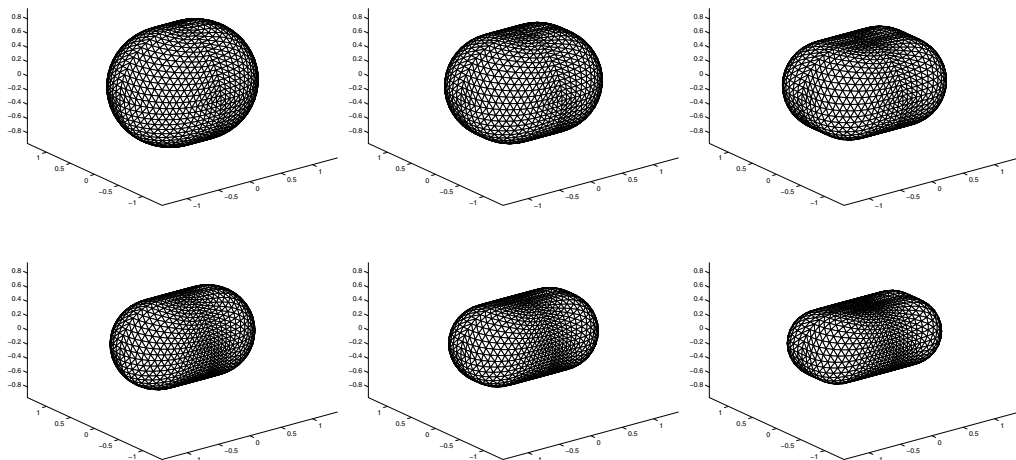


Figure 2. Sphere-Cylinder-Plane-element (SCyPe) example shapes: upper row, aspect ratios $b/a = c/a = 0.8$ (left), $b/a = 0.8$ and $c/a = 0.7$ (middle), $b/a = 0.8$ and $c/a = 0.6$ (right); lower row, $b/a = c/a = 0.6$ (left), $b/a = 0.60$ and $c/a = 0.525$ (middle), $b/a = 0.60$ and $c/a = 0.45$ (right).

where ϕ_1 and ϕ_2 denote the azimuths of the terminators on the cylindrical envelope and

$$\begin{aligned}
 C_1 &= (\epsilon'_x l'_x - \epsilon'_y l'_y) \cos 2\tilde{\phi} + (\epsilon'_x l'_y + \epsilon'_y l'_x) \sin 2\tilde{\phi}, \\
 C_2 &= -(\epsilon'_x l'_x - \epsilon'_y l'_y) \sin 2\tilde{\phi} + (\epsilon'_x l'_y + \epsilon'_y l'_x) \cos 2\tilde{\phi}, \\
 C_3 &= \epsilon'_x l'_x \sin^2 \tilde{\phi} + \epsilon'_y l'_y \cos^2 \tilde{\phi} - (\epsilon'_x l'_y + \epsilon'_y l'_x) \sin \tilde{\phi} \cos \tilde{\phi}.
 \end{aligned} \tag{4.6}$$

Finally, in order to compute the total disk-integrated brightness adhering to the SCyPe model, the various rotations need to be accounted for. The present numerical implementations have been carefully checked both internally and against other independent implementations to compute disk-integrated brightnesses.

The statistical inversion of observed photometric brightnesses for spins and shapes is carried out by sampling the spin parameters and by fitting the shape parameters for each trial spin solution. When the trial spin-shape solution provides a statistically acceptable fit to the observations, it qualifies for a sample solution. Obtaining a large number of sample solutions allows one to characterize the solution space within the present SCyPe model. The complete probabilistic treatment requires, additionally, the derivation of weights for the sample solutions.

It is clear that SCyPe will not generally lead to rms fits as good as those from conventional inversion (Kaasalainen, Torppa & Muinonen (2001), Kaasalainen, Mottola & Fulchignoni (2002), Torppa (1999)). However, the application of SCyPe models is some two orders of magnitude faster than the application of the conventional methods.

4.2. Results

In the case of the previously observed Apollo asteroids – (1685) Toro, (1981) Midas, and (1862) Apollo – the amount of data is large enough for using the conventional inversion technique. All three objects represent moderate albedos (Toro and Midas as S-type and Apollo as Q-type). The previous photometric observations were extracted from Standard Asteroid Photometric Catalog SAPC <http://www.astro.helsinki.fi/SAPC/>. We have compared our results to the previous ones available at the European Asteroid Research

Node's (EARN) Near-Earth Asteroid Database (<http://earn.dlr.de/nea/>), which is an update and extension of that by Binzel, Lupishko, Di Martino, *et al.* (2002). For the four new objects (2002 FF₁₂, 2003 MS₂, 2003 RX₇, 2004 HW), the spin and shape were studied using SCyPe.

In what follows, we summarize the results for the NEOs included in this paper, with pole directions in ecliptic longitude λ and latitude β :

(1685) *Toro*

In addition to the two new curves from this observing program, we used one unpublished curve observed with the La Silla Danish 1.54-m telescope and ten previously observed lightcurves by Dunlap, Gehrels & Howes (1973). There exist also five lightcurves from 1988 by Hoffmann & Geyer (1990), but it was impossible to get a good fit when they were combined with either the Dunlap data or our NOT and La Silla observations. Also, since the new lightcurves are from the same view point and observing geometry as Hoffmann and Geyer's data, we left the latter unused. There were thus 13 lightcurves available from a time interval of 31 years. The Earth-centered ecliptic longitude of Toro ranges 15° for NEON observations and 80° for Dunlap's observations. No unambiguous pole solution could be obtained, and the distribution of the possible spin states was obtained using the conventional inversion method. Results with rms error greater than 0.03 mag can be discarded due to the high accuracy of the data. The pole latitude was constrained to negative values, i.e., retrograde rotation, whereas the pole longitude is restricted to $\lambda \in [250^\circ, 120^\circ]$. Except for the period, the previous pole solution by Dunlap, Gehrels & Howes (1973) ($\beta = 55^\circ$, $\lambda = 200^\circ$ and $P = 10.196$ h) disagrees with our findings.

(1862) *Apollo*

For the analysis of Apollo, we used 23 previously observed lightcurves by Harris, Young, Goguen, *et al.* (1987) and Hahn (1983) (UAPC), two unpublished curves from the Ondrejov NEO program (Pravec, Wolf & Šarounová (1998)), and one new lightcurve from this program. The Earth-centered ecliptic longitude of the previously observed data sets range 65° and 85° , and the new curve from the NOT observations as well as the Ondrejov curves provide information from two more view points. The total time range of the observations increased to 25 years along with the new lightcurve, thus increasing also the accuracy of the period solution. We used the conventional inversion method for the data analysis, and one spin solution produced clearly the best fit with an rms of 0.036 mag being of the same order as the noise of the data. Spin values for this solution were $\beta = -50^\circ$, $\lambda = 20^\circ$, and $P = 3.0662$ h, which is not far from the previous solution $\beta = -26^\circ$, $\lambda = 56^\circ$ and $P = 3.065$ h by Harris, Young, Goguen, *et al.* (1987). Although the two rms minima in the period plot are equal, the difference becomes larger when fitting the final shape model. The nominal shape solution is shown in Fig. 3 – the detailed error analysis is left for the future.

(1981) *Midas*

For the analysis of Midas, we used six previously observed lightcurves: one by Wisniewski, Michalowski, Harris *et al.* (1997) and five by Mottola, de Angelis, di Martino *et al.* (1995). The two new lightcurves from this program increased the total time range of the observations to 18 years, and the number of observing geometries to three. A distribution for the possible spin solutions was obtained using the conventional inversion method. The former period solution is 5.22 hours (Wisniewski, Michalowski, Harris *et al.* (1997) and Mottola, de Angelis, di Martino *et al.* (1995)), which is in the error bars of the one (5.215 ± 0.035 h) obtained by us. In terms of rms of the fits, there exist no clear

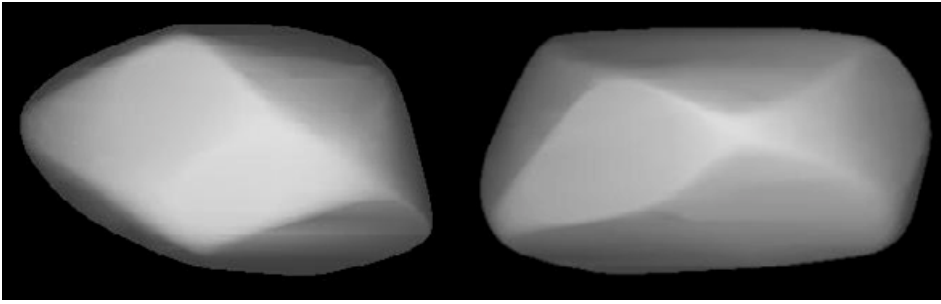


Figure 3. Convex shape model for (1862) Apollo (Torppa, Virtanen & Muinonen *et al.* (2006)).

minima. Due to the low accuracy of the data, we have to accept all the solutions below the rms-value of 0.04 mag.

2002 FF₁₂

We had one 5.8-h lightcurve of 2002 FF₁₂, which by chance covers at least part of one maximum. From these data we can see only by inspecting the lightcurve, without any specific model, that the period is most probably more than 8.5 hours. The SCyPe method was applied including also period determination with sampling from 8 to 20 h. The forbidden regions in the pole space turn out to be small. The shape is not constrained either and values up to 0.95 are allowed for the aspect ratios due to the small amplitude of the lightcurve (0.3 mag). However, the dependence of the shape on the pole direction is noted. The smallest rms values are obtained with periods from nine to ten hours, but the distribution is flat and values larger than ten hours have to be taken into account as well.

2003 MS₂

We observed one 5.9-h lightcurve of 2003 MS₂ (Fig. 4), and the period according to this is approximately 7 hours. The distribution of possible spin-axis solutions obtained with the SCyPe model are also depicted in Fig. 4. There are two large forbidden regions in β vs. λ : the possible solutions are constrained into two narrow rings around the forbidden regions. Note that the density of the points does not correspond to the probability of the solution. In addition, the shape is quite well constrained due to the large amplitude of the lightcurve (0.7 mag); maximum value for b/a is 0.67. However, since only one curve, assumingly over one rotation, was available for the analysis, one must be cautious when using these spin and shape estimates for further studies. The results are described in more detail in Torppa, Virtanen & Muinonen *et al.* (2006); with the present pilot study, we want to show that it is indeed possible to derive information about an object from a small amount of data.

2003 RX₇

We observed one 6-hour lightcurve of 2003 RX₇, which shows a period of about 2.6 hours. The SCyPe method was applied to obtain distributions of the spin and shape parameters. The results are quite similar to those of 2002 FF₁₂, but the forbidden regions in β vs. λ are more clear. The amplitude of the lightcurve is 0.2 mag, and thus the aspect ratios are allowed to obtain values up to 0.92. Best-fit solutions are distributed evenly all over the region of possible solutions.

2004 HW

Five lightcurves of 2004 HW were observed showing the period of 2.52 hours. In the curve observed on Sept. 15, we see an increasing trend in the magnitude. This may be

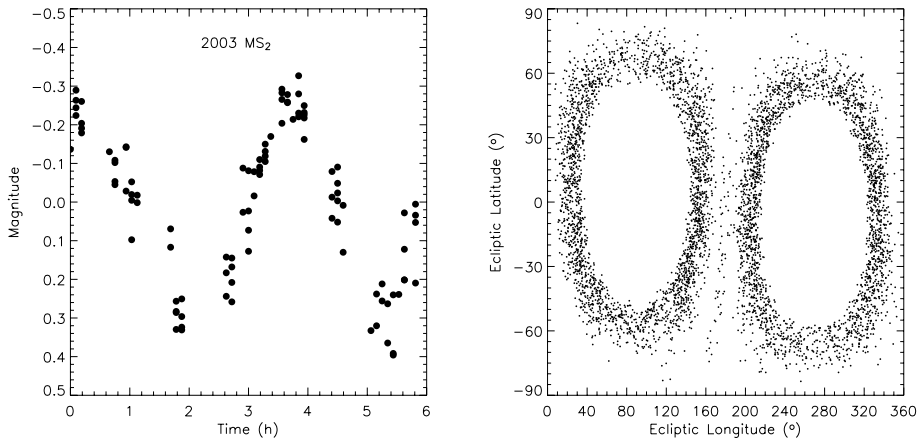


Figure 4. Relative R-filter photometry (left) and spin-axis solutions for 2003 MS₂ (right).

due to a satellite (cf. Pravec, Harris & Warner (2006); or cometary activity), since no change in magnitude should be present due to scattering behaviour; the change in phase angle at epoch of observations was 0.5° per day. The lightcurves were observed within a short time (one month apart), and a distribution of possible pole and shape solutions was obtained by applying the SCyPe method. Best-fit solutions settle mostly around pole longitudes $\lambda = 200^\circ$ and $\lambda = 20^\circ$. Shape is strongly dependent on the pole solution.

5. Conclusions

We have reviewed the progress of the NEON program for characterizing physical and dynamical properties of potentially hazardous near-Earth objects. Observations at the Nordic Optical Telescope have resulted in improved understanding of the spins, shapes, and orbits of a number of near-Earth objects. In particular, R-filter relative magnitudes have been obtained for a considerable number of objects, keeping the door open for an absolute calibration in the future.

A novel statistical method based on SCyPe shape models (Sphere-Cylinder-Plane-element) has been outlined for the inversion of spins and shapes from photometric observations, allowing for detailed error analyses. Furthermore, SCyPe modeling can allow the optimization of future photometric observations. The forbidden zones from single lightcurves suggest that the subsequent observations could be made at ecliptic longitudes and latitudes covered by the permissible zones. If such observational circumstances are available, one may obtain additional constraints on the pole orientation.

Acknowledgements

We thank the Nordic Optical Telescope (NOT) and Dk1.54 for granting us observing time. Most of the data utilized have been obtained using ALFOSC, which is owned by the Instituto de Astrofísica de Andalucía (IAA) and operated at the Nordic Optical Telescope under agreement between IAA and the NBIFAFG of the Astronomical Observatory of Copenhagen. The study has been funded by Vilho, Yrjö and Kalle Väisälä foundation, the Academy of Finland, and the Finnish Graduate School in Astronomy and Space Physics. Finally, we would like to thank the anonymous reviewer for constructive criticism.

References

- Alvarez-Candal, A., Duffard, R., Angeli, C. A., Lazzaro, D., & Fernandez, S. 2004, *Icarus* 172, 388
- Binzel, R. P., Lupishko, D. F., Di Martino, M., Whiteley, R. J., & Hahn, G. J. 2002, in: W. F. Bottke, A. Cellino, P. Paolicchi, R. P. Binzel (eds.), *Asteroids III* (University of Arizona Press), p. 255
- Bowell, E., Virtanen, J., Muinonen, K., & Boattini, A. 2002, in: W. F. Bottke, A. Cellino, P. Paolicchi, R. P. Binzel (eds.), *Asteroids III* (University of Arizona Press), p. 27
- Dunlap, J. L., Gehrels, T. & Howes, M. L. 1973, *Astron. J.* 78, 491
- Granvik, M. & Muinonen K. 2005, *Icarus* 179, 109
- Hahn, G. 1983, in: C.-I. Lagerkvist, H. Rickman (eds.), *Asteroids, Comets, Meteors* (Uppsala University), p. 35
- Harris, A. W., Young, J. W., Goguen, J., Hammel, H. B., Hahn, G., Tedesco, E. F., Tholen, D. J., *et al.* 1987, *Icarus* 70, 246
- Hoffmann, M. & Geyer, E. H. 1990, *Acta Astronomica* 40, 389
- Kaasalainen, M. 2004, *A&A* 426, 1103
- Kaasalainen, M. & Torppa, J. 2001, *Icarus* 153, 24
- Kaasalainen, M., Torppa, J. & Muinonen, K. 2001, *Icarus* 153, 37
- Kaasalainen, M., Mottola, S. & Fulchignoni, M. 2002, in: W.F. Bottke, A. Cellino, P. Paolicchi, R.P. Binzel (eds.), *Asteroids III* (University of Arizona Press), p. 139
- Lagerkvist, C.-I., Piironen, J. & Erikson A 2001, *Uppsala Asteroid Photometric Catalogue*, Fifth update (Uppsala Astronomical Observatory)
- Mottola, S., de Angelis, G., di Martino, M., Erikson, A., Hahn, G. & Neukum, G. 1995, *Icarus* 117, 62
- Muinonen, K. 1998, *A & A* 332, 1087
- Muinonen, K. & Bowell, E. 1993, *Icarus* 104, 255
- Muinonen, K., Virtanen, J. & Bowell, E. 2001, *Cel. Mech. Dyn. Astron.* 81(1), 93
- Muinonen, K., Virtanen, J., Granvik, M., & Laakso, T. 2005, in: *Proceedings of the symposium Three Dimensional Universe with Gaia* (ESA SP-576), p. 223
- Muinonen, K, Virtanen, J., Granvik, M., & Laakso, T. 2006, *MNRAS* 368, 809
- Parviainen, H. & Muinonen, K. 2006, *J. Quantit. Spectrosc. Radiat. Transf.*, in press
- Pravec, P., Wolf, M., & Šarounová, L. 1998, *Icarus* 136, 124
- Pravec, P., Harris, A. W. & Warner, B. 2006, in: A. Milani, G. B. Valsecchi, D. Vokrouhlický (eds.), *Proceedings of the IAU Symposium 236: Near-Earth Objects, our Celestial Neighbors: Opportunity and Risk*, in press
- Raab H. 2004, *Astrometrica*, <http://www.astrometrica.at/>
- Tedesco, E., & Zappalà, V. 1980, *Icarus* 43, 33
- Torppa J., 1999, *Asteroid lightcurve inversion: methods for obtaining a unique and stable shape solution*, MSc thesis, Univ. Helsinki
- Torppa, J. & Muinonen, K. 2005, in: *Proceedings of the symposium Three Dimensional Universe with Gaia* (ESA SP-576), p. 321
- Torppa, J., Kaasalainen, M., Michalowski, T., Kwiatkowski, T., Kryszczyńska, A., Denchev, P., & Kowalski, R. 2003, *Icarus* 164, 346
- Torppa, J., Virtanen, J., Muinonen, K., Laakso, T., Niemelä, J., Näränen, J., Aksnes, K., Dai, Z., Lagerkvist, C.-I., Rickman, H., Hahn, G., Michelsen, R., Grav, T., Pravec, P., & Jørgensen, O. G. (2006), *Icarus*, submitted
- Virtanen, J. 2005, *Asteroid orbital inversion using statistical methods*, PhD thesis (University of Helsinki)
- Virtanen, J. & Muinonen, K. 2006, *Icarus* 184, 289
- Virtanen, J., Muinonen, K. & Bowell, E. 2001, *Icarus* 154, 412
- Virtanen, J., Tancredi, G., Muinonen K., & Bowell, E. 2003, *Icarus* 161, 419
- Virtanen, J., Muinonen, K., Granvik, M., Laakso, T. 2005, in: Z. Knežević & A. Milani (eds.), *Proceedings of IAU Colloquium 197: Dynamics of Populations of Planetary Systems*, p. 239
- Virtanen, J., Tancredi, G., Bernstein, G. M., Spahr, T., & Muinonen, K. 2006, in: A. Barucci, H. Boehnhardt, D. Cruikshank, A. Morbidelli (eds.), *Kuiper Belt*, submitted
- Wisniewski, W. Z., Michalowski, T. M., Harris, A. W., & McMillan, R. S. 1997, *Icarus* 126, 395